Biological Journal of the Linnean Society, 2021, **XX**, 1–10. With 5 figures.

Cranial integration in the ring-necked parakeet, *Psittacula krameri* (Psittaciformes: Psittaculidae)

MATTHEW J. MITCHELL[1,2,*], ANJALI GOSWAMI[1] and RYAN N. FELICE[2]

[1]*Department of Life Sciences, Natural History Museum, Cromwell Road, Kensington, London, SW7 5BD, UK*
[2]*Centre for Integrative Anatomy, Department of Cell and Developmental Biology, University College London, Gower Street, Bloomsbury, London, WC1E 6BT, UK*

Received 30 December 2020; revised 11 February 2021; accepted for publication 13 February 2021

The study of integration and modularity aims to describe the organization of components that make up organisms, and the evolutionary, developmental and functional relationships among them. Both have been studied at the interspecific (evolutionary) and intraspecific (phenotypic and ontogenetic) levels to different degrees across various clades. Although evolutionary modularity and integration are well-characterized across birds, knowledge of intraspecific patterns is lacking. Here, we use a high-density, three-dimensional geometric morphometric approach to investigate patterns of integration and modularity in *Psittacula krameri*, a highly successful invasive parrot species that exhibits the derived vertical palate and cranio-facial hinge of the Psittaciformes. Showing a pattern of nine distinct cranial modules, our results support findings from recent research that uses similar methods to investigate interspecific integration in birds. Allometry is not a significant influence on cranial shape variation within this species; however, within-module integration is significantly negatively correlated with disparity, with high variation concentrated in the weakly integrated rostrum, palate and vault modules. As previous studies have demonstrated differences in beak shape between invasive and native populations, variation in the weakly integrated palate and rostrum may have facilitated evolutionary change in these parts of the skull, contributing to the ring-necked parakeet's success as an invasive species.

ADDITIONAL KEYWORDS: birds – disparity – modularity – morphology – parrots – phenotypic integration – skull.

INTRODUCTION

Although an organism must function as a complete integrated whole in order to survive, the component parts of that organism can in fact grow, function and evolve semi-independently from one another. This phenomenon is described by modularity: the degree to which collections of organismal traits form independently varying and evolving units (Olson & Miller, 1958; Klingenberg, 2009). The covariation between modules or among traits within a module, termed 'integration', arise from their genetic, developmental and functional associations (Olson & Miller, 1958). By quantifying aspects of integration and modularity such as strength, pattern and change over time, it is possible to gain insight into the functional, genetic and developmental systems that give rise to this variation (Felice *et al.*, 2019a).

The relationship between the magnitude of phenotypic integration and the evolution of phenotypic variation is complex and seems to vary across clades and systems. In the archosaur skull some aspects of evolutionary integration are consistent across a wide range of taxa (such as high integration in the occipital region), and some parts of cranial integration vary greatly between groups. These differences are exhibited in the patterns of integration between the quadrate, pterygoid and jugal in birds and non-avian dinosaurs (Felice *et al.*, 2019a). Previous work has suggested that variation in integration and modularity may impact phenotypic evolution and explain differences in evolutionary patterns observed across taxa (Cheverud, 1996). In carnivorans and

*Corresponding author. E-mail: matthew.mitchell.19@ucl.ac.uk

primates, high levels of integration have been found to constrain disparity, restricting evolution by limiting the extent and direction in which selection can act on variation (Goswami & Polly, 2010). In some cases, however, the opposite effect is observed. In the felid axial skeleton, higher integration appears to facilitate greater response to selection (Randau & Goswami, 2017). Some studies have found no evidence of a relationship between strength of integration and disparity at all (Bardua *et al.*, 2019a).

Recent research has begun to reveal the complex relationships among cranial traits in birds (Bright *et al.*, 2016, 2019; Felice & Goswami, 2018; Navalón *et al.*, 2020). Some studies have found the avian cranium to be highly modular, with modules of differing degrees of integration evolving at different rates. Some believe that this leads to a range of highly specialized species and that high-level modularity is associated with high evolutionary rate and low disparity (Felice & Goswami, 2018; Felice *et al.*, 2019a). Others attribute the highly specialized forms seen in some birds to a more highly integrated pattern of modularity (Bright *et al.*, 2019). Research that features honeycreepers and Darwin's finches, for example, suggests that high levels of integration between the rostrum and the rest of the skull are associated with a high rate of evolution (Navalón *et al.*, 2020). Finally, some studies have found that allometry (the relationship between shape and size) is a significant predictor of variation in the cranium (Klingenberg, 2016; Bright *et al.*, 2019). The results of these investigations of evolutionary integration are often interpreted as a reflection of the correlations imparted by the shared underlying developmental systems that generate variation in these traits. To truly understand the link between evolutionary integration and developmental/population scale phenomena requires quantifying phenotypic integration at intraspecific scales. However, although studies into intraspecific integration and modularity are becoming more common (Marshall *et al.*, 2019; Bon *et al.*, 2020 and see Parr *et al.*, 2016), investigations in birds are still lacking. Here, we quantify cranial integration and modularity in a single species of parrot, the ring-necked parakeet, to test whether evolutionary integration is indeed a reflection of population-scale integration patterns.

The Psittaciformes (parrots) is an order containing approximately 390 species (del Hoyo *et al.*, 2020), split into three 'superfamilies' of the Psittacoidea ('true' parrots), the Cacatuoidea (cockatoos) and the Strigopoidea (New Zealand parrots). Parrots exhibit a set of cranial novelties that include a vertical palate, ossified arcus suborbitalisas and a pseudoprokinetic cranio-facial hinge that is thought to provide increased agility and a greater range of movement (Tokita, 2003). It has been argued that this adaption is key to their survival as it allows them to access the mechanically restrictive food that they require, although this is debated (Tokita, 2003; Bright *et al.*, 2016).

Studies investigating evolutionary patterns of integration and modularity in parrots provide support for several competing hypotheses of modularity in the skull. Felice & Goswami (2018) found a high level of modularity across bird species (including the Psittaciformes), with different modules evolving at different rates. Furthermore, this study proposed that the unique palate in parrots is a self-contained module that has evolved independently at a higher rate than other parts of the skull (Felice & Goswami, 2018). Other research, however, suggests that rather than high modularity, high levels of allometry and integration throughout the parrot cranium explain the majority of variation observed (Bright *et al.*, 2019). Methodologies can differ greatly in their approaches to measuring shape data: Felice & Goswami (2018) did not control for allometry and used a high-density landmark approach, which is typically less influenced by allometric effects (Goswami *et al.*, 2019). Allometric effects can be considerable regardless of the degree of modularity, especially within less inclusive clades where size-related variation may dominate. Given the size of the Psittaciformes order and variation within it, it is therefore likely that allometry has a stronger effect within the Psittaciformes than across all birds (Bright *et al.*, 2016, 2019; Klingenberg *et al.*, 2016; Marshall *et al.*, 2019).

Evolutionary (interspecific) patterns of modularity and integration often replicate static (intraspecific) patterns (Klingenberg, 2014), although in some taxa this is not the case (Urošević *et al.*, 2012). In the fire salamander, intraspecific modularity patterns closely match results of studies investigating intraspecific variation in caecilians, as well as interspecific patterns across the wider caecilians clade, despite osteological differences (Bardua *et al*, 2019a; Marshall *et al.*, 2019; Bon *et al.*, 2020). In contrast, cranial analysis in squamates appears to vary across the taxa; research focussing on evolutionary integration has revealed high levels of modularity across the clade (Watanabe *et al.*, 2019), whereas research investigating static integration has found the cranium to be more integrated (Urošević *et al.*, 2012). It has been suggested that a strong degree of static integration is associated with function and the more modular evolutionary patterns are more influenced by development; this implies that functional modularity can be adaptive (Urošević *et al.*, 2019).

Here, we investigate static patterns of modularity and morphological integration in the cranium of the ring-necked parakeet, *P. krameri*, using a high-density geometric morphometric approach. Our aim is to investigate the roles of integration and

modularity in the evolution of the specialized skull of the Psittaciformes order and determine whether patterns of phenotypic integration and modularity in this species reflect those of studies of evolutionary integration in birds. We test 13 different hypotheses (Supporting Information, Table S1) concerning the organization of nine cranial regions, based on results found in studies of avian evolutionary modularity. Furthermore, we investigate the influence of allometric size on cranial shape and integration and quantify the relationship between morphological diversity and within-module integration. We predict that the skull of the ring-necked parakeet will show high levels of modularity, with individual skull regions showing distinct patterns of disparity and within-module integration. Our results will enable us to compare and contrast intraspecific variation within this particular species with interspecific variation between other parrots, among birds and with tetrapods in general.

MATERIAL AND METHODS

Specimens and data collection

The sample consisted of 37 alcohol-preserved adult specimens of *P. krameri* of unknown sex and age, retrieved from the collection of the Natural History Museum (NHM) at Tring, Hertfordshire, UK. A full list of specimens can be found in the Supporting Information (Table S2). Specimens were scanned using a Nikon Metrology X-Tek HMX ST 225 micro-CT scanner at NHM, London, UK. Tomographs were processed into surface files using Avizo Lite v.9.3 (FEI, Hillsboro, OR, USA) before being imported into Geomagic Wrap 2017 (3D Systems, Inc. Rock Hill, South Carolina, USA), where the lower mandible and postcranial skeleton were removed and any artefactual holes filled. Based on suture development, all specimens appeared to be sexually mature. Before being exported from Geomagic Wrap, the 'decimation' tool was used to reduce the specimen to under one million faces to reduce the file size without compromising quality of detail. Some specimens that had been damaged on the right-hand side were mirrored using the 'flip' function in Geomagic, so the same side of each specimen could be used for landmarking (Supporting Information, Table S2).

Morphometric analysis

Landmarks (Type I and II) and semilandmark curves were placed by a single researcher (M.J.M.) using Stratovan Checkpoint (Stratovan, Davis, CA, USA). Landmarks were placed bilaterally and semilandmark curves were placed on the right side only (Fig. 1; Supporting Information, Tables S3, S4). The skull was split into nine different regions, with landmarks and semilandmark curves used to define each area (Fig. 1; Supporting Information Tables S3, S4). Shape data were imported into RStudio v.1.1.419 running R v.3.6.1. (R Core Development Team, 2020) and landmarks and semilandmarks were checked thoroughly before conducting any analysis. Any landmarks that could not be placed due to damage to the skull were marked as 'missing data' in Checkpoint and coordinates were estimated

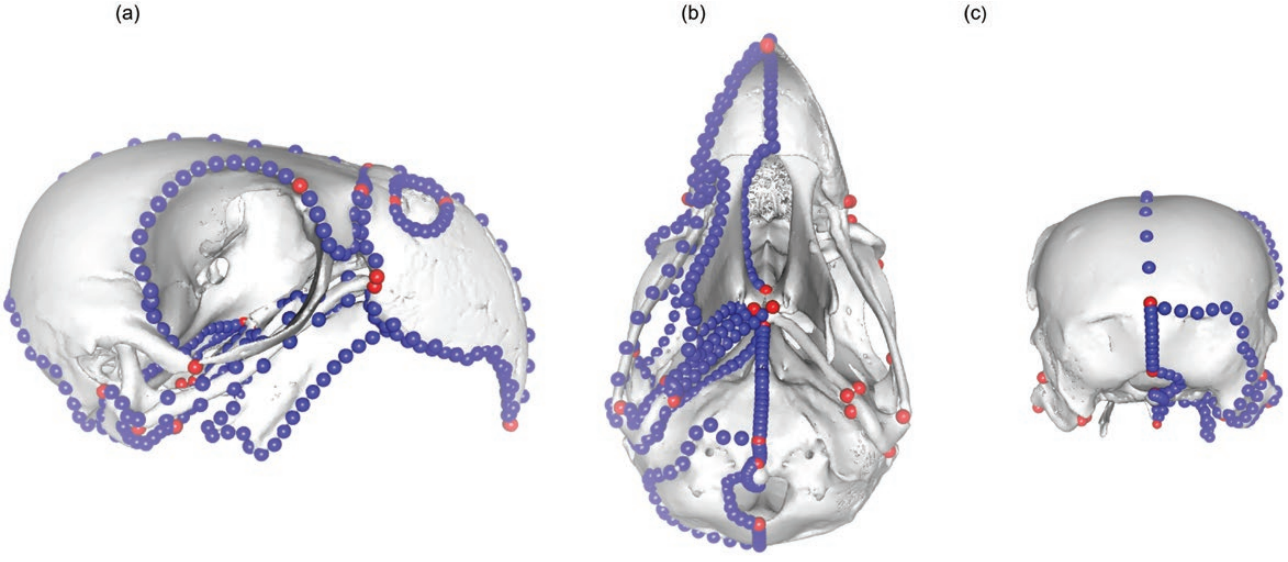

Figure 1. Anatomical landmarks (blue) and semilandmark curves (red) applied to each specimen, shown here on specimen 25. a, lateral view; (b) inferior view; (c) posterior view.

using the 'estimate.missing' function of the package *geomorph* v.3.2.1 (Adams *et al.*, 2020; Supporting Information, Table S2). Curves were subsampled to a consistent number of points across specimens (Supporting Information, Table S4).

The 'createAtlas' function of *morpho* v.2.8 (Schlager, 2017) was used to create a template of the surface semilandmarks on a hemisphere model. The 'placePatch' function of *morpho* v.2.8 (Schlager, 2017) was used to project surface semilandmarks from the model onto the surface of the cranium of each specimen using 'inflate' and 'tol' values that were optimized for each region (Bardua *et al.*, 2019b; Supporting Information, Table S5). The patch data from each part of the cranium were then combined so that the right side of each specimen was fully covered in patch points (Bardua *et al.*, 2019b). The 'slider3D' function of *morpho* v.2.8 (Schlager, 2017) was used to slide the landmarks along the curves and surfaces of the skull to minimize bending energy (Gunz *et al.*, 2005). We then used the 'mirrorfill' function of *paleomorph* v.0.1.4 (Lucas & Goswami, 2017) to mirror landmarks from the right side of the skull over to the left, by linking any landmarks on the left side to their corresponding right-hand side landmarks. Mirroring landmarks aimed to remove any potential artefacts caused by Procrustes analysis when applied to only one side of the skull (Cardini, 2016). Some surface semilandmarks were consistently projected onto the wrong part of the skull; these were removed, leaving a total of 38 anatomical landmarks, 24 curves and 384 patch points placed onto each specimen (Supporting Information, Tables S3–S5). We then carried out a generalized Procrustes alignment on our morphometric data using the 'gpagen' function of *geomorph* v.3.2.1 (Adams *et al.*, 2020) to remove the non-biological variation caused by differences in translation and rotation, as well as isometric scaling. Mirrored landmarks were then removed before further analysis.

Allometry

To estimate the influence of allometry on shape variation in our data set, we fit permutational linear regressions using the 'procD.lm' function of *geomorph* v.3.2.1 (Adams *et al.*, 2020), using skull centroid size as the size value and 1000 permutations.

Principal components analysis

A principal components analysis (PCA) was conducted on the shape data using the 'PlotTangentSpace' function of *geomorph* v.3.2.1 (Adams *et al.*, 2020) to determine the main axes of shape variation within the data set and explore the distribution of specimens in morphospace. The 'plotRefToTarget' function of *geomorph* v.3.2.1 (Adams *et al.*, 2020) was then used to warp a specimen to represent the extremes of PC1 and PC2 to help visualize the data.

Modularity and integration

We tested 13 different hypotheses for modularity, from maximum modularity of nine modules (rostrum, naris, jugal, vault, quadrate, basisphenoid, pterygoid, occipital and palate) to a layout of just two: the face and neurocranium (Supporting Information, Table S1). Modularity was tested using both the 'Evaluating Modularity with Maximum Likelihood' (EMMLi) and Covariance Ratio (CR) methods. Firstly, the 'dotcorr' function of *paleomorph* v.0.1.4 (Lucas & Goswami, 2017) was used to determine the correlation between landmarks. The 'EMMLi' function of the *EMMLi* v.0.0.3 package (Goswami *et al.*, 2017) used these correlations to compare the different hypotheses and calculate the between-module and within-module integration for each module of each hypothesis. Because EMMLi may prefer overparameterized models, we then conducted a CR analysis using the 'modularity.test' function of *geomorph* v.3.2.1 (Adams *et al.*, 2020) to quantify support for the two best-supported hypotheses by testing which showed the higher modular signal. This approach quantifies the strength of modularity by comparing between-module covariance to within-module covariance (Adams, 2016). Each modularity test was run with 1000 iterations. The 'compare.CR' function of *geomorph* v.3.2.1 (Adams *et al.*, 2020) was used to compare the results of these tests.

Morphological variance

We used the 'morphol.disparity' function of *geomorph* v.3.2.1 (Adams *et al.*, 2020) to quantify the variance within each module. The result was used to investigate the relationship between the Procrustes variance and within-module integration (calculated from EMMLi) for each module. We also used the 'per_lm_variance' function of the hot.dots package v.0.0.0.9 (Felice *et al.*, 2018) to calculate the per-landmark variance of each individual landmark on the cranium, allowing us to visualize the distribution of variation across the entire skull.

RESULTS

Allometry

The effect of centroid size on shape of the *P. krameri* skull was not significant ($R^2 = 0.025$, $P = 0.586$). As such, no correction for the effects of allometric size were made for subsequent analyses.

Principal component analysis

The PCA of the cranium identified 36 principal components (PCs) that together explained 100% of the variation of the cranium; 95% of the variance was explained by PC1-PC28. The main axis of variation was represented by PC1, which exhibited 19.7% of the total variation, mostly describing variation in the depth of the curve of the cranial vault, the circumference of the orbit and the length and curvature of the rostrum. PC2 represented 9.5% of the total variation and was driven by variation in the width and curvature of the underside of the rostrum as well as the shape of the quadrate (Fig. 2).

Modularity and integration

EMMLi

The most supported hypothesis from the EMMLi analysis was the maximum modularity hypothesis (Supporting Information, Tables S1, S6). This suggests that all nine defined regions of the skull (rostrum, naris, jugal, vault, quadrate, basisphenoid, pterygoid, occipital and palate) are independent modules. Highest between-module integration was found between the rostrum and naris, and the pterygoid and occipital (Fig. 3). The highest within-module integration was found in the pterygoid (Fig. 3; Table 1). Within-module integration was greater than between-module integration for all nine modules.

Covariance ratio

The modularity.test for the 'all modules' hypothesis (nine distinct cranial modules) produced a CR score of 0.624 (P = 0.001). The modularity test for the seven-module hypothesis [e.g. the hypothesis supported in Felice & Goswami (2018)] showed a slightly higher CR score of 0.642 (P = 0.001), signalling less support. When 'compare.CR' was used to compare support for the hypotheses, the nine-module hypothesis was found to have the stronger signal (z-score of -28.4 compared to -28.0, P = 0.037). These results support those of the EMMLi analysis, that the nine-module hypothesis best reflects the pattern of integration within *P. krameri*.

Morphological variance

The rostrum, cranial vault and palate showed the highest morphological disparity (Procrustes variance), with the lowest disparity found in the naris (Table 1). A linear regression between Procrustes variance and within-module integration found a significant negative relationship, suggesting that as within-module integration increases, morphological variance decreases (adjusted R^2 = 0.705, P = 0.0284; Fig. 4). Most per-landmark variance was found in landmarks around the edge of the orbital, the tip of the rostrum, the palate, and also on the ventral posterior of the cranium between the orbital and the occipital region (Fig. 5).

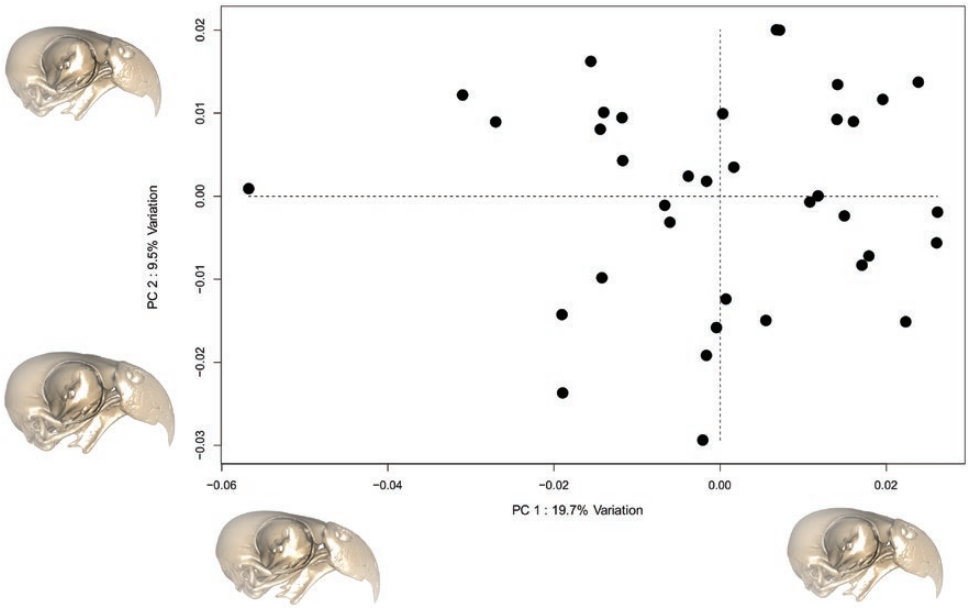

Figure 2. Morphological space showing the distribution of specimens according to variation described by PC1 and PC2. PC1 represented 19.7% of variation and PC2 represented 9.5%.

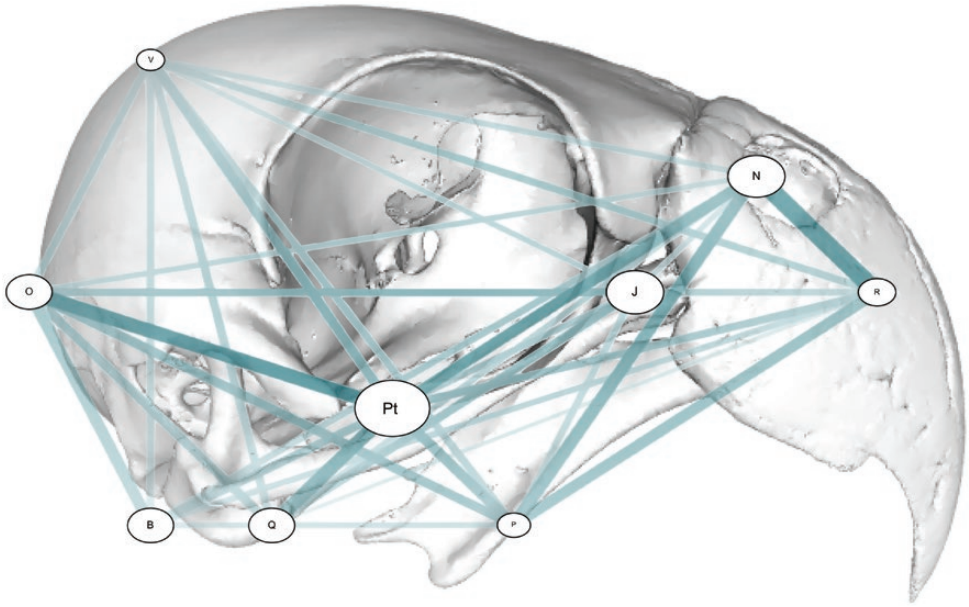

Figure 3. Network graph showing the results of the EMMLi analysis; degrees of the within-module and between-module integration in the *P. krameri* cranium. Circle size represents within-module integration and the thickness of the connective bars represents the degree of between-module integration. B: Basisphenoid region, J: Jugal, N: Naris, O: Occipital region, P: Palate, Pt: Pterygoid, Q: Quadrate, R: Rostrum, V: Vault.

Table 1. Procrustes variance ($\times 10^{-4}$) and within-module integration for each of the nine cranial regions, as well as within-module integration scores calculated using EMMLi

Anatomical region	Procrustes variance ($\times 10^{-4}$)	Within-module integration
Rostrum	1.19	0.37
Jugal	0.31	0.61
Palate	1.67	0.34
Pterygoid, ventral surface	0.54	0.73
Quadrate, articular surface	0.69	0.51
Basisphenoid	0.73	0.45
Occipital region	0.97	0.50
Cranial vault	1.69	0.32
Naris	0.26	0.59

DISCUSSION

P. krameri exhibits a pattern of high modularity in the skull. From 13 hypotheses representing different patterns of modularity between the nine major cranial regions, both EMMLi and CR analyses found most support for our hypothesis of maximal modularity, suggesting that the cranium of *P. krameri* is split up into nine distinct modules. This provides evidence that the evolution of the unique cranial features possessed by parrots may be the result of each region of their cranium being a highly integrated subunit that can respond to selection and evolve somewhat independently from the others.

This pattern of phenotypic integration, found from measuring an intraspecific data set, can be compared to the results of evolutionary (interspecific) studies of integration and modularity in birds to determine whether evolutionary patterns replicate those we observed here at the intraspecific level. Felice & Goswami (2018) studied evolutionary integration and modularity in a wide range of birds and found the avian cranium to be highly modular, albeit with a slightly different pattern. Their results show the pattern of modularity in the avian cranium to be made up of seven modules, using the same modularity pattern used here, but with the rostrum and jugal combined as one module and the pterygoid and quadrate combined as one module. Importantly, this seven-module hypothesis was the hypothesis of maximal modularity in their study: no nine-module hypothesis was defined (Felice & Goswami, 2018). Here, we directly compared our hypothesis of maximal modularity (nine modules) with their most supported hypothesis of seven modules using compare CR, and found that our nine-module hypothesis had significantly more support.

Other studies have found higher levels of cranial integration in birds. Navalón *et al.* (2020) aimed to determine the relationship between beak and skull

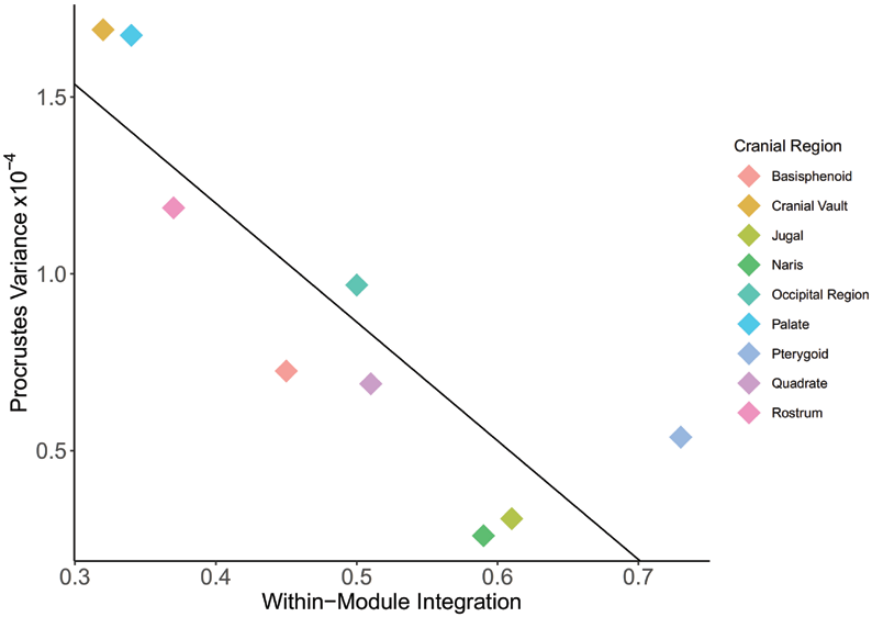

Figure 4. The relationship between within-module integration and disparity. A linear regression found a significant negative effect (adjusted $R^2 = 0.7052$, $P = 0.0284$). Line: $y = -3.359x + 2.543$.

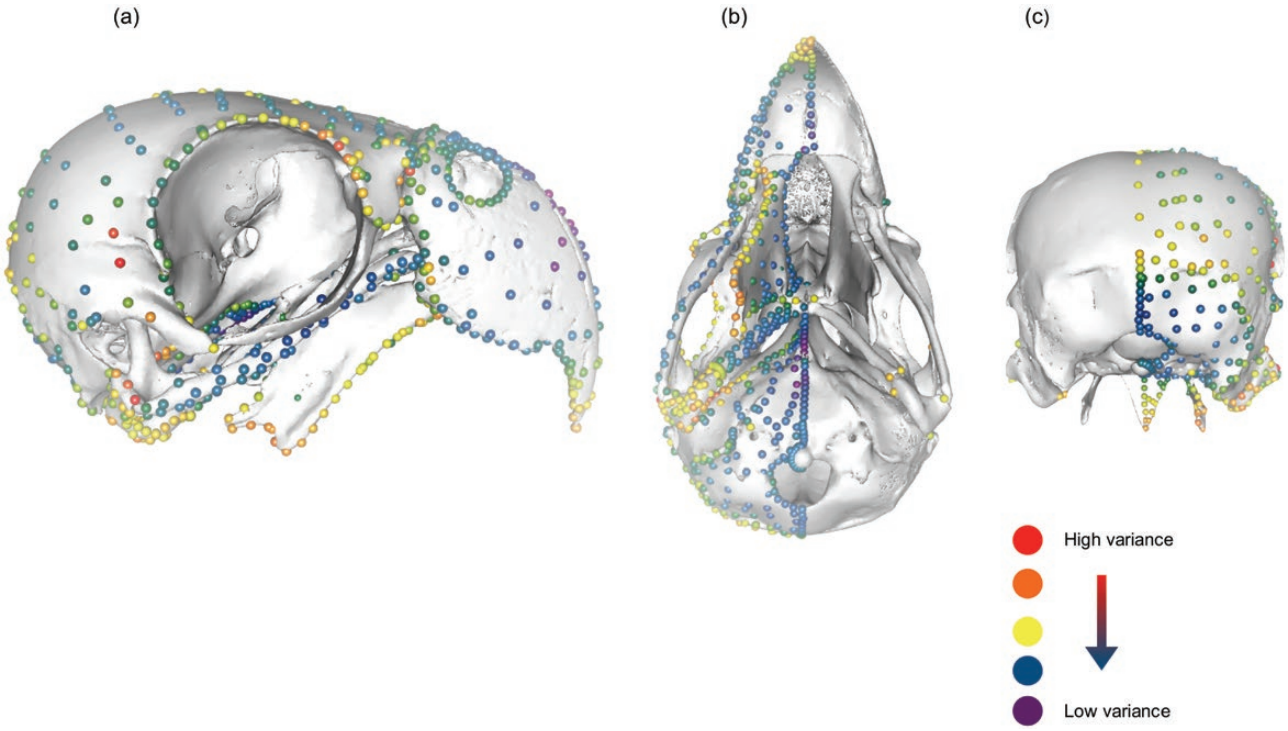

Figure 5. Hot dots analysis projected onto specimen 25. 'Hotter' colours represent a greater degree of variation in a specific landmark compared to 'colder' colours, which show less. Most variation can be seen around and behind the orbital, around the palate and on the quadrate. a, lateral view; (b) inferior view; (c) posterior view.

shape in land birds. They focussed on Hawaiian honeycreepers and Darwin's finches, two species thought to show high modularity in those areas. Unexpectedly, their results showed that integration was high between the beak and the rest of the skull, and that the whole cranium played a part in the fast

evolution associated with these species (Navalón *et al.*, 2020). They found these results unique among land birds and concluded that both a high degree of modularity and a high degree of integration can facilitate evolution (Navalón *et al.*, 2020). Bright *et al.* (2019) used different methods to find that variation in the skull was explained by significant allometry and identified high levels of integration between beak shape and skull shape.

A key reason for these differences in findings across integration and modularity studies could be the types of data and methods used. Bright *et al.* (2019) used an approach consisting of 20 landmarks across the midline and the right-hand side of the skull as well as semilandmark curves along the dorsal midlines of the beak and skull. Here, we used a similar high-density landmark approach to Felice & Goswami (2018) with considerably more anatomical landmarks and curves as well as surface landmarks that span the whole of the right side of the cranium. Previous research has found that results from only using anatomical landmark data (or limited curves) can vary from results that use surface patching approaches; results from a landmark-only data set may emphasize between-region correlations over within-region integration because landmarks are concentrated at the borders of regions, whereas surface semilandmarks sample between boundaries (Goswami *et al.*, 2019; Bon *et al.*, 2020). The consequence of this is that results from landmark-only analyses often show considerably weaker support for more modular organizations (boundary bias), simply because they primarily capture shape information at the most integrated regions of elements: their boundaries (Goswami *et al.*, 2019). Moreover, Bright *et al.* (2016, 2019) did not specifically test alternate modular structures, but rather measured the integration between the two regions of interest, the beak and braincase.

In further contrast to Bright *et al.* (2016, 2019), we also found no significant effect of allometry in our data set. This is likely because we were studying a single species rather than two different groups of parrots. As the superfamilies Psittacoidea and Cacatuoidea vary so greatly [and were both included in the study by Bright *et al.* (2019)], a more comparable study to ours would investigate whether allometry has any effect on an intraspecific data set consisting of cockatoos only or a different species of Psittacoidea.

We also recover a negative relationship between Procrustes variance and within-module integration, implying that high integration within modules restricts disparity. These results mirror research into evolutionary integration in bird taxa that have found high levels of cranial-wide integration restrict variance (Felice & Goswami, 2018). We found particularly high variance within the palate and rostrum of our specimens (as well as low within-module integration), implying that these modules have a high degree of variation and therefore a potentially high evolutionary rate (Felice & Goswami, 2018). These results reflect those found studying birds and certain other mammalian taxa such as carnivorans and primates (Goswami & Polly, 2010; Felice & Goswami, 2018), although this complex relationship appears to vary across clades. For example, no consistent relationship between disparity and within-module integration has been identified in squamates (Watanabe *et al.*, 2019) or various clades of amphibians (Bardua *et al.*, 2019b, 2020; Fabre *et al.*, 2020).

High levels of variation in the palate and rostrum may be linked to the ring-necked parakeet's success as an invasive species. A previous study investigating the differences between morphology of populations of ring-necked parakeets in their native range and the invasive populations that inhabit Europe has found that the beaks of those in non-native ranges tend to be bigger and stronger (Le Gros *et al.*, 2016). The palate and rostrum are directly involved in feeding, so high variation in two specific modules may have helped the species adapt to a new environment and food source more easily. Thus, selection on specific beak morphologies may have been facilitated by high levels of rostrum and palate variation within the species, though the relationship between diet and skull shape is complex (Bright *et al.*, 2019; Felice *et al.*, 2019b). These results are in line with the hypothesis that high modularity can facilitate broad ecological tolerances and thus rapid invasion of new habitats (Adams *et al.*, 2007). However, the integration and modularity patterns observed here in *P. krameri* are similar to those seen in all birds (Felice & Goswami, 2018). Direct comparison between this cosmopolitan taxon and related parrot species that are vulnerable to climate change or habitat loss are needed to test how cranial modularity might influence ecological flexibility and niche conservatism in this clade.

Using a three-dimensional approach, we analysed cranial shape and patterns of modularity and integration in *P. krameri*, the ring-necked parakeet, finding a highly modular pattern consisting of nine internally integrated modules. We found a significant negative relationship between within-module integration and disparity that mirrors results from analyses of evolutionary integration in the avian skull using high-density geometric morphometrics. Our findings support the hypothesis that high levels of modularity can facilitate the development of specialized cranial features that enable organisms to adapt to new ecological niches. Amongst parrots, our findings suggest that this high degree of modularity has facilitated the evolution of the unique palate and cranio-facial hinge that are

distinctive to their cranium. The palate and rostrum modules both show a low degree of within-module integration (Fig. 4), implying relaxed constraint. This low integration in turn leads to greater variation in these regions and provides greater opportunity for natural selection to act on them, allowing them to evolve independently into their specialized forms. It may also facilitate higher evolutionary rates than in a more integrated system (Felice & Goswami, 2018). To determine whether this effect is found more widely, further investigation could compare this intraspecific data set with intraspecific data sets of other parrots (particularly cockatoos) as well as other birds. Building on the results of this analysis and macro-scale analyses across birds, further studies into interspecific integration patterns that compare species across the Psittaciformes would clarify the role integration and modularity play in the specialization of the parrot cranium and in the evolutionary diversity and success of both native and invasive populations.

ACKNOWLEDGEMENTS

We would like to thank Vincent Fernandez at NHM, London for providing access to and assistance with the CT scanner, and also Jeffrey W. Streicher, Andrew Knapp and two anonymous reviewers for providing valuable feedback on the written manuscript. We would also like to thank Carla Bardua, Ellen Coombs, Anne-Claire Fabre, Lucy C. Huntley and Sarah Cockerill for help with software and general support. This work was funded by European Research Council grant STG-2014–637171 to AG. The authors declare no conflicts of interest.

REFERENCES

Adams DC. 2016. Evaluating modularity in morphometric data: challenges with the RV coefficient and a new test measure. *Methods in Ecology and Evolution* **7:** 565–572.

Adams DC, **Collyer ML**, **Kaliontzopoulou A. 2020.** *Geomorph: software for geometric morphometric analyses. R package Version 3.2.1.* Available at: https://cran.r-project.org/package=geomorph

Adams DC, **West ME**, **Collyer ML. 2007.** Location-specific sympatric morphological divergence as a possible response to species interactions in West Virginia *Plethodon* salamander communities. *Journal of Animal Ecology* **76:** 289–295.

Bardua C, **Fabre AC**, **Bon M**, **Das K**, **Stanley EL**, **Blackburn DC**, **Goswami A. 2020.** Evolutionary integration of the frog cranium. *Evolution; International Journal of Organic Evolution* **74:** 1200–1215.

Bardua C, **Felice RN**, **Watanabe A**, **Fabre A-C**, **Goswami A. 2019a.** A practical guide to sliding and surface semilandmarks in morphometric analyses. *Integrative Organismal Biology* **1:** obz016.

Bardua C, **Wilkinson M**, **Gower DJ**, **Sherratt E**, **Goswami A. 2019b.** Morphological evolution and modularity of the caecilian skull. *BMC Evolutionary Biology* **19:** 30.

Bon M, **Bardua C**, **Goswami A**, **Fabre A-C. 2020.** Cranial integration in the fire salamander, *Salamandra salamandra* (Caudata: Salamandridae). *Biological Journal of the Linnean Society* **4:** 1129–1140.

Bright JA, **Marugán-Lobón J**, **Cobb SN**, **Rayfield EJ. 2016.** The shapes of bird beaks are highly controlled by nondietary factors. *Proceedings of the National Academy of Sciences of the United States of America* **113:** 5352–5357.

Bright JA, **Marugán-Lobón J**, **Rayfield EJ**, **Cobb SN. 2019.** The multifactorial nature of beak and skull shape evolution in parrots and cockatoos (Psittaciformes). *BMC Evolutionary Biology* **19:** 104.

Cardini A. 2016. Lost in the other half: improving accuracy in geometric morphometric analyses of one side of bilaterally symmetric structures. *Systematic Biology* **65:** 1096–1106.

Cheverud JM. 1996. Developmental integration and the evolution of pleiotropy. *American Zoologist* **36:** 44–50.

Fabre AC, **Bardua C**, **Bon M**, **Clavel J**, **Felice RN**, **Streicher JW**, **Bonnel J**, **Stanley EL**, **Blackburn DC**, **Goswami A. 2020.** Metamorphosis shapes cranial diversity and rate of evolution in salamanders. *Nature Ecology & Evolution* **4:** 1129–1140.

Felice RN, **Goswami A. 2018.** Developmental origins of mosaic evolution in the avian cranium. *Proceedings of the National Academy of Sciences of the United States of America* **115:** 555–560.

Felice RN, **Randau M**, **Goswami A. 2018.** A fly in a tube: macroevolutionary expectations for integrated phenotypes. *Evolution; International Journal of Organic Evolution* **72:** 2580–2594.

Felice RN, **Watanabe A**, **Cuff AR**, **Noirault E**, **Pol D**, **Witmer LM**, **Norell MA**, **O'Connor PM**, **Goswami A. 2019a.** Evolutionary integration and modularity in the archosaur cranium. *Integrative and Comparative Biology* **59:** 371–382.

Felice RN, **Tobias JA**, **Pigot AL**, **Goswami A. 2019b.** Dietary niche and the evolution of cranial morphology in birds. *Proceedings. Biological Sciences* **286:** 20182677.

Goswami A, **Lucas T**, **Sivasubramaniam P**, **Finarelli J. 2017.** *EMMLi: a maximum likelihood approach to the analysis of modularity. R package Version 0.0.3.* Available at: https://cran.r-project.org/package=EMMLi

Goswami A, **Polly PD. 2010.** The influence of modularity on cranial morphological disparity in Carnivora and Primates (Mammalia). *PLoS One* **5:** e9517.

Goswami A, **Watanabe A**, **Felice RN**, **Bardua C**, **Fabre AC**, **Polly PD. 2019.** High-density morphometric analysis of shape and integration: the good, the bad, and the not-really-a-problem. *Integrative and Comparative Biology* **59:** 669–683.

Gunz P, **Mitteroecker P**, **Bookstein FL. 2005.** Semilandmarks in three dimensions. In: Slice DE, ed. *Modern morphometrics in physical anthropology*. New York: 73–98.

del Hoyo J, **Elliott A**, **Sargatal J**, **Christie DA**, **Kirwan G. 2020.** *Handbook of the birds of the World alive*. Barcelona: Lynx Edicions. Available at: http://www.hbw.com/ (retrieved 06/05/2020).

Klingenberg CP. 2009. Morphometric integration and modularity in configurations of landmarks: tools for evaluating a priori hypotheses. *Evolution & Development* **11:** 405–421.

Klingenberg CP. 2014. Studying morphological integration and modularity at multiple levels: concepts and analysis. *Philosophical Transactions of the Royal Society of London. Series B, Biological Sciences* **369:** 20130249.

Klingenberg CP. 2016. Size, shape, and form: concepts of allometry in geometric morphometrics. *Development Genes and Evolution* **226:** 113–137.

Le Gros A, **Samadi S**, **Zuccon D**, **Cornette R**, **Braun MP**, **Senar JC**, **Clergeau P. 2016.** Rapid morphological changes, admixture and invasive success in population of ring-necked parakeets (*Psittacula krameri*) established in Europe. *Biological Invasions* **18:** 1581–1598.

Lucas T, **Goswami A. 2017.** *paleomorph: geometric morphometric tools for paleobiology. R package Version 0.1.4.* Available at: https://cran.r-project.org/package=paleomorph

Marshall AF, **Bardua C**, **Gower DJ**, **Wilkinson M**, **Sherratt E**, **Goswami A. 2019.** High-density three-dimensional morphometric analyses support conserved static (intraspecific) modularity in caecilian (Amphibia: Gymnophiona) crania. *Biological Journal of the Linnean Society* **126:** 721–742.

Navalón G, **Marugán-Lobón J**, **Bright JA**, **Cooney CR**, **Rayfield EJ. 2020.** The consequences of craniofacial integration for the adaptive radiations of Darwin's finches and Hawaiian honeycreepers. *Nature Ecology & Evolution* **4:** 270–278.

Olson EC, **Miller RL. 1958.** *Morphological integration*. Chicago: University of Chicago Press.

Parr WCH, **Wilson LAB**, **Wroe S**, **Colman NJ**, **Crowther MS**, **Letnic M. 2016.** Cranial shape and the modularity of hybridization in dingoes and dogs; hybridization does not spell the end for native morphology. *Evolutionary Biology* **43:** 171–187.

R Core Development Team. 2020. *R: a language and environment for statistical computing*. Vienna: R Foundation for Statistical Computing. Available at: https://www.R-project.org/

Randau M, **Goswami A. 2017.** Unravelling intravertebral integration, modularity and disparity in Felidae (Mammalia). *Evolution & Development* **19:** 85–95.

Schlager S. 2017. Morpho and Rvcg—shape analysis in R. In: Zheng G, Li S, Szekely G, eds. *Statistical shape and deformation analysis*. Cambridge: Academic Press, 217–256.

Tokita M. 2003. The skull development of parrots with special reference to the emergence of a morphologically unique cranio-facial hinge. *Zoological Science* **20:** 749–758.

Urošević A, **Ljubisavljević K**, **Ivanović A. 2019.** Multilevel assessment of the Lacertid lizard cranial modularity. *Journal of Zoological Systematics and Evolutionary Research* **57:** 145–158.

Urošević A, **Ljubisavljević K**, **Jelić D**, **Ivanović A. 2012.** Variation in the cranium shape of wall lizards (*Podarcis* spp.): effects of phylogenetic constraints, allometric constraints and ecology. *Zoology* **115:** 207–216.

Watanabe A, **Fabre AC**, **Felice RN**, **Maisano JA**, **Müller J**, **Herrel A**, **Goswami A. 2019.** Ecomorphological diversification in squamates from conserved pattern of cranial integration. *Proceedings of the National Academy of Sciences of the United States of America* **116:** 14688–14697.

SUPPORTING INFORMATION

Additional Supporting Information may be found in the online version of this article at the publisher's web-site:

Table S1. Modularity patterns of different hypotheses tested.
Table S2. List of specimens used, along with any relevant notes. All specimens were retrieved from the collections at the Natural History Museum (NHM), Tring, UK.
Table S3. Locations of anatomical landmarks used.
Table S4. Locations of semilandmarks used.
Table S5. Areas of the skull that were patched, the number of patch points used per area and details on semi-automated landmarking parameters.
Table S6. Results from EMMLi analyses including model parameters, raw log-likelihood fits and AICc scores for all tested models.

SHARED DATA

3D models are available for download on www.phenome10k.org